Regular Article

Design, Synthesis and Antiproliferative Activities of Oxidative Stress Inducers Based on 2-Styryl-3,5-dihydro-4*H*-imidazol-4-one Scaffold

Abdelsattar M. Omar,*[a,b,#] Tamer M. Abdelghany,[c] Mohamed S. Abdel-Bakky,[c,d] Abdulrahman M. Alahdal,[a] Mohamed F. Radwan,[a,e] and Moustafa E. El-Araby*[a,f,#]

[a] *Department of Pharmaceutical Chemistry, Faculty of Pharmacy, King Abdulaziz University; Jeddah 21589, Saudi Arabia:* [b] *Department of Pharmaceutical Chemistry, Faculty of Pharmacy, Al-Azhar University; Cairo 11884, Egypt:* [c] *Department of Pharmacology, Faculty of Pharmacy, Al-Azhar University; Cairo 11884, Egypt:* [d] *Department of Pharmacology, Faculty of Pharmacy, Aljouf University; Aljouf 74331, Saudi Arabia:* [e] *Department of Medicinal Chemistry, Faculty of Pharmacy, Minia University; Minya 61519, Egypt: and* [f] *Department of Pharmaceutical Organic Chemistry, Faculty of Pharmacy, Helwan University; Cairo 11790, Egypt.*

Received May 25, 2018; accepted July 18, 2018; advance publication released online July 25, 2018

The 2-styryl-3,5-dihydro-4*H*-imidazol-4-one might be considered as a system with isosteric properties similar to *trans*-cinnamaldehyde (styrylaldehyde), a safe natural compound that exhibited interesting activities against various cancers. We synthesized a series of compounds that differ structurally in having different alkyl, aryl and heterocyclic substituents at the N3 position of the 2-styryl-4-imidaolone pharmacophore. The compounds were assayed for their cytotoxicity against both cancer and normal cell lines. In addition, their cellular mechanism of action as reactive oxygen species (ROS) inducers were investigated. Many of the synthesized compounds showed higher activities on colon, breast and hepatic cancer cell lines than the parent *trans*-cinnamaldehyde. Compounds 3a and 3e showed selective antiproliferative activity against cancer cell lines at low micromolar to sub-micromolar IC_{50} value. Compounds were extremely less toxic on normal cell lines baby hamster kidney fibroblasts (BHK) and human lung tissue fibroblast (WI-38). Similar to *trans*-cinnamaldehyde, the colon cancer cell cycle analysis indicated cell cycle changes consistent with increased oxidative stress leading to apoptosis. Compound 3e caused elevation of all cell oxidative indicators of ROS such as a decrease in reduced glutathione, increased malondialdehyde and suppression of catalase and superoxide dismutase activities. Dihydroethidium staining, nuclear fragmentation and increased caspase-3 further confirmed extensive apoptotic induction due to ROS accumulation upon treatment of human colon adenocarcinoma (HCT116) cells with compounds 3a and 3e. Changes in human breast adenocarcinoma (MCF7) cells were less revealing for ROS induction and increased oxidative stress. Conclusion: The compounds represent an example of efficient rescaffolding of a natural compound to a highly potent drug-like analogues.

Key words selective antiproliferative; reactive oxygen species; redox dysregulation; oxidative stress marker; imidazolone; colon cancer

4-Imidazolones (3,5-Dihydro-4*H*-imidazol-4-one) bearing arylidene at C-5 position and variety of substituents on positions N-3 and C-2 (Fig. 1) is a synthetically accessible heterocyclic scaffold that has been studied as a potential anticancer[1–3] with other therapeutic benefits.[4–8] Moreover, this nucleus exists in the marine alkaloid rhopaladins A–D which was found to exert some interesting biological activities.[9] The versatility of 4-imidazolones attracted our attention during our quest to identify compounds with potential anticancer activities. For instance, we discovered promising antiproliferative activities of some 4-imidazolone derivatives such as Cur-3 (Fig. 1) against colon cancer cell lines during our reported research on multi-drug resistance modulating agents.[3]

From another prespective, it was established that natural small molecules constitute a valuable source of new leads in anticancer drug discovery because they are usually characterized by low toxicities and intriguing activities.[10] For instance, *trans*-cinnamaldehyde (tCA), the major constituent of cinnamon bark extract, has been extensively investigated for its activities against various cancer cells such as colon, breast, liver, melanoma and leukemia (see review by Hong *et al.*).[11] Induction of oxidative stress *via* increased reactive oxygen species (ROS) has been reported as a major mechanism for the apoptotic effect of tCA and its closely related derivatives such as 2′-benzyloxycinnamaldehyde (BCA)[12,13] (Fig. 1). tCA and its derivatives were found to exert a pro-oxidant effect leading to elevated ROS as they also decreased the functional levels of the anti-oxidant cellular components such as glutathione (GSH) and thioredoxin reductase.[14] It has been established that heightened ROS levels generate an oxidative stress on cancer cells and induce apoptosis on cancer cells.[15] However, ROS elevation in healthy normal cells may lead to increased oxidative stress associated with inflammatory and oncogenic disorders.[16] Fortunately, the oxidative stress caused by tCA and its analogues apparently has more influence on cancer than normal cells as they were found to activate the antioxidant nuclear factor-E2-related factor 2 (Nrf2)/Keap1-antioxidant response element (ARE) signaling pathway in non-immortalized primary fetal colon cells.[17] Regardless of its ROS-elevating properties, tCA is recognized by the U.S. Food and Drug Administration (FDA) as a safe food supplement and flavor.[18,19] On the downside, tCA is an aldehyde with a high metabolic conversion rate and poor pharmacokinetics and it is not suitable for drug development.[20,21] In this report, we aimed to synthesize and investigate cytotoxic properties of 2-styryl-4-imidazolone series of compounds incorporating the

[#] These authors contributed equally to this work.

* To whom correspondence should be addressed. e-mail: asmansour@kau.edu.sa; madaoud@kau.edu.sa

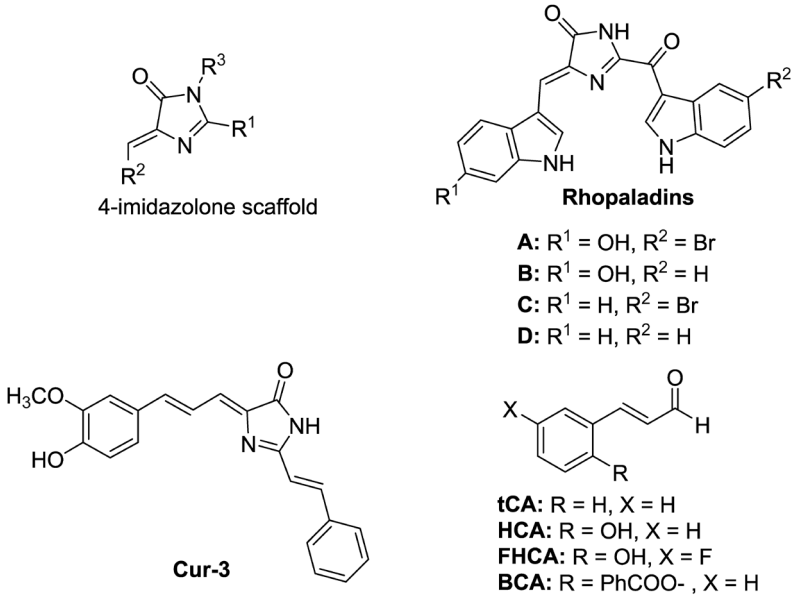

Fig. 1. Imidazol-4-one Scaffold, Its Derivatives Alkaloid Rhopaladins and Cur-3 (Cytotoxic Agent)

In the bottom-left side, the structure of *trans*-cinnamaldehyde and its derivatives that have proven cytotoxic activities against cancer cell lines.

styryl portion of the tCA.

Results

Design and Chemical Synthesis Chemically, 4-imidazolones are electron-withdrawing heterocycles because they contain a conjugated carbonyl system. Therefore, we hypothesized that appending a styryl group C-2 of 4-imimidazole would possibly retain the antiproliferative cytotoxic activity of tCA acting by similar cellular mechanisms of tCA. In theory, heterocyclic 4-imidazolone may resist metabolic conversion more than easily oxidized aldehydes. More importantly, from prior experience it has been shown that 4-imidazolone derivatives were able to produce *in vivo* activities against inflammation and convulsions.[4,22] Since this work is a first step to explore the potentiality of 2-styryl-4-imidazolne as anticancer surrogates, a systematic approach was followed for deciding the list of compounds to prepare. Fixing the group at the 4-postion as benzylidene and variation of amines at the N-5 of the imidazolone ring aimed to achieve the activity target (Fig. 2).

The compounds were synthesized starting from cinnamoylglycine **1** which was condensed with benzaldehyde according to standard Erlenmeyer procedure to give the azlactone **2**, a known intermediate, that was then reacted with different aliphatic, aromatic and heterocyclic amines to produce the desired imidazolones **3a**–**m**[4] (Chart 1).

The stereochemistry of the benzylidene group at position 5 is an established (*Z*) isomer according to literature reports on similar cases.[9] The compounds were fully characterized and purities were confirmed using spectral analyses (NMR, LC/MS) in addition to elemental analyses.

The amines selected for the final step in the chart varied from aliphatic (**3b**, **3m**), to phenyl (**3b**), substituted phenyl (**3c**, **3d**, **3e**, **3f**), heterocyclic (**3i**, **3j**, **3k**, **3l**, **3m**) or arylalkyl (**3h**, **3l**), in addition to the unsubstituted N-5 analogue (**3a**). Moreover, the compound set covered a range of polar to nonpolar substituents as well as variable electron densities on the aromatic rings according to the varied N-3 substituents.

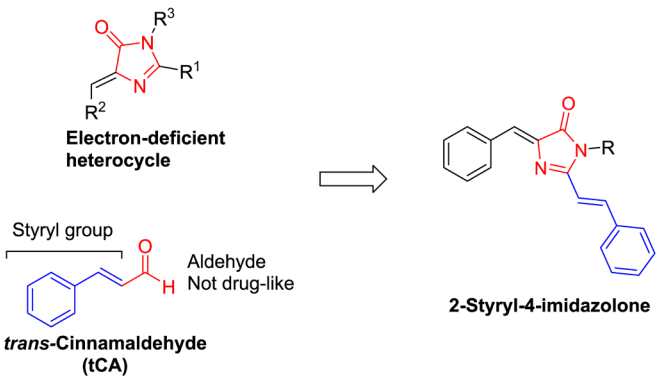

Fig. 2. Design of Imidazolone Derivatives as tCA Mimics

(Color figure can be accessed in the online version.)

Our first objective in this research was to identify cytotoxic compounds with an acceptable level of potency ($<5\,\mu$M). Once this step was accomplished, we aimed to study cellular mechanisms, aiming to confirm apoptosis induction *via* ROS elevation in a similar way to the natural lead tCA[11] and its derivatives.[12,23] In addition, potency against not only cancer cell lines, but also against normal, highly proliferative mammalian cells were sought as an indicator of electivity and preliminary toxicity.[24]

Biological Screening

Cytotoxicity and Cell Cycle Arrest

All compounds were screened for their cytotoxic activity using sulforhodamine B (SRB)[25] assay against three different cancer cell lines: human colon adenocarcinoma (HCT116), human breast adenocarcinoma (MCF7) and human hepatocellular carcinoma (HepG2). These cell lines represent the most common spread of malignant diseases. The majority of our compounds exhibited significant growth inhibition of cancer cells against all three cancer cell lines (Table 1). For example, compounds **3a**, **3c**, **3e** and **3m** showed universal cytotoxic activities ranged from 0.5 to 4.0 μM IC_{50} values. Generally,

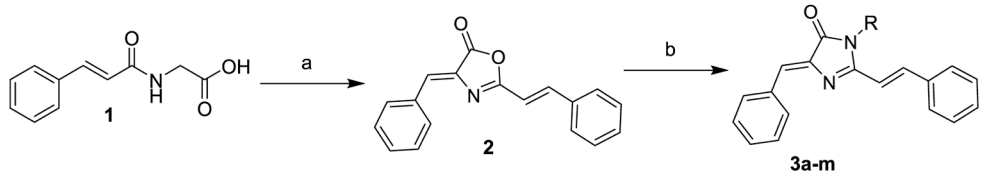

(a) Benzaldehyde, acetic anhydride, heat, 15 min, yield 65%; (b) RNH_2, acetic acid, sodium acetate, heating 70–80°C, yield 16–74%.

Chart 1. Synthesis of Imidazolone Derivatives **3a**–**m**

Table 1. Cytotoxic Effect of Imidazolone Derivatives on CRC (HCT116), Breast (MCF7) and Hepatic (HepG2) Cancer Cell Line.

Cpd No.	R	IC_{50}±S.E. (μM)				
		HCT116	MCF-7	HepG2	BHK	WI-38
3a	H	3.6±2.19	3.15±1.5	2.93±2	777±27	>1000
3b	*n*-Pr	9.8±1.44	24.6±1.5	0.7±1.4	>1000	>1000
3c	Ph	2.7±1.5	1.8±1.6	3.2±1.9	>1000	>1000
3d	4-F-Ph	35.2±1	35.16±1.2	30.6±5.8	>1000	>1000
3e	4-OH-Ph	0.49±3.9	3.9±1.8	3.7±2.1	524±21	363±17
3f	3-CN-Ph	3.2±1.8	18.7±1.16	0.39±1.9	693±25	>1000
3g	3-CF_3-Ph	12.1±1.7	21±1.08	28.8±5.3	>1000	>1000
3h	Bn	13.7±1	23.2±1.7	4.2±1	33.1±1.1	66.5±5.8
3i	3-Pyridyl	79.8±1.5	37.1±1.5	43.18±1.5	>1000	>1000
3j	5-Methyl-2-thiazolyl	16.3±1.17	31.4±1.5	2.2±2.3	749.2±38	>1000
3k	2-(1,3,4-Thidiazolyl)	29.15±5	7.8±4	11.8±3.5	>1000	>1000
3l	Furfuryl	28.6±4.6	2.6±1.6	3.5±1.8	65.0±1.4	60.9±6.5
3m	2-(4-Morpholinyl)ethyl	2.5±2.9	2.6±1.37	2.2±1.2	53.3±1.12	45.5±2.8
2		10.5±1.1	17.45±1.3	14.4±1.7	>1000	584±105
tCA		12.4±1.2	8.8±2	>100	63.9±13	40.8±1.5

The last two columns are cytotoxic activities on two normal (non-cancerous) highly proliferative cell lines: baby hamster kidney fibroblasts (BHK); and diploid human cell lines (WI-38). IC_{50} values are calculated as the concentration that kills 50% of the cell population employing SRB assay; Data are presented as means±standard error of the mean.

many of the tested compounds had higher cytotoxic activities than the lead tCA. Some compounds showed selective inhibition against a certain cell line. In this regard, compounds **3b**, **3h** and **3j** showed more potent activities against HepG2 than HCT116 or MCF7. The 3-(3-cyanophenyl)imidazolone derivative (**3f**) was clearly a selective inhibitor of HCT116. The antiproliferative activities of many imidazolones **3** were higher than the isosteric oxazolone **2**.

The synthesized compounds demonstrated differential activity towards cancer cell lines over normal (non-cancerous cell lines). The selectivity test was performed by inhibition assay against two types of normal highly proliferative cell lines: Baby hamster kidney fibroblasts (BHK) and Diploid Human WI-38 cells. For instance, the potent anticancer compound **3a** killed cancer cells of colon, breast and liver at IC_{50} values at 3.6, 3.15 and 2.96 respectively. This compound was remarkably safe to the normal cells as illustrated in Fig. 3. Compounds **3a** and **3e** had no appreciable toxic activity on both BHK and WI-38 cell lines as their selectivity index against cancer cells was found to be more than 100 times over normal cells. Some of the screened compounds (**3h**, **3l** and **3m**) showed lower selectivity as they inhibited BHK and WI-38 cell lines with IC_{50} values less than 100 μM.

The changes in the cell cycle profile were found to be time dependent as the distribution of the percentage of cells population in each stage varied considerably from zero h (control) to 24 to 48 h (Fig. 4). In HCT116, the cytotoxic compounds **3a** and **3e** caused non-significant changes on the Pre-G phase cell

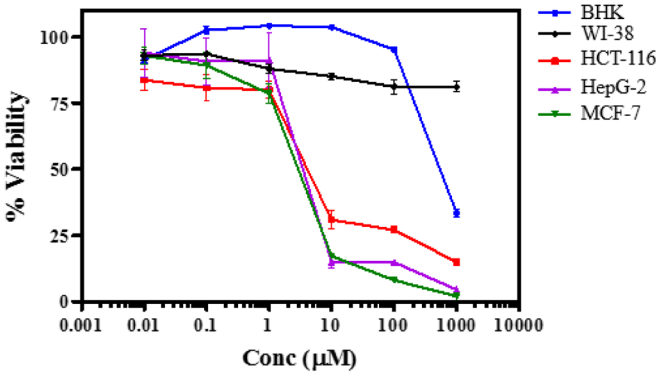

Fig. 3. Dose–Response Curves of Cytotoxic Effect of Compound **3a** on Normal Cell Lines: BHK (Blue) and WI-38 (Black); In Addition to Cancer Cell Lines: HCT-116 (Red), HepG-2 (Purple) and MCF-7 (Green)

(Color figure can be accessed in the online version.)

population compared to control after 24 h. On the other hand, the 48 h treatment resulted in a dramatic increase in the percentage of cells at Pre-G by 4 and 5 folds, respectively compared to control. Moreover, both compounds induced a significant increase in the S-phase population with a concomitant decrease in the G0/G1 population, indicating S-phase arrest.

The changes in the Pre-G phase were less clear in MCF7 cells for all three tested compounds **3a**, **3c** and **3m**. Furthermore, longer time incubation of **3c** did not result in an increase in Pre-G, while all three compounds increased the

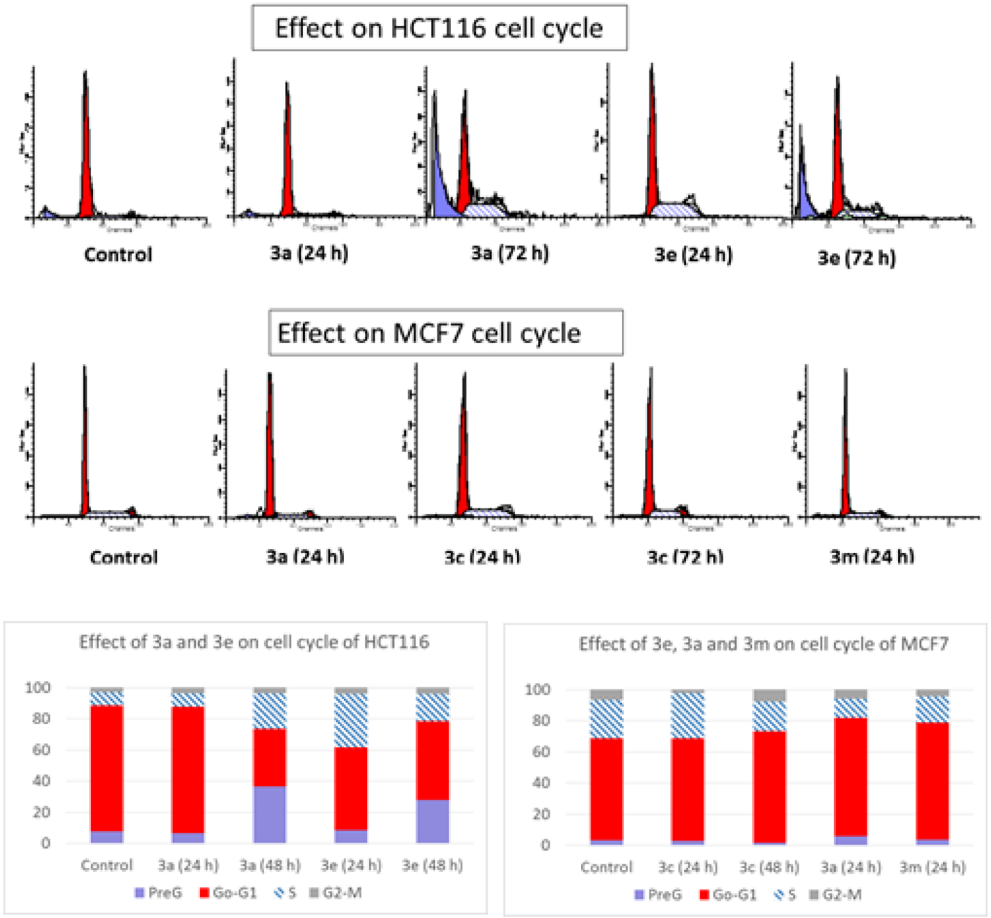

Fig. 4. Effect of Compounds **3a**, **3e**, **3c**, and **3m** on Cell Cycle Distribution of HCT116 and MCF7 Cell Lines

(Color figure can be accessed in the online version.)

population of cells at G0/G1 phase. This may indicate that these compounds might act through a different mechanism on MCF7 than HCT116 cell lines.

Mechanisms of Cytotoxicity in HCT116 Cells

In order to further investigate the mechanism of cytotoxicity of the universally potent compounds, we conducted different experiments on the compounds **3a** and **3e**. The two compounds were expected to induce apoptosis of cancer cells by oxidative stress and downstream consequences similar to tCA due to their above mentioned design.

To study the effect of **3a** and **3e** on free radical generation and oxidative stress induction, HCT116 cells were incubated with the IC_{50} of compounds **3a** and **3e** for 48 h. At the end of the incubation period, the cell lysates were assayed for the content of redox regulators. Both compounds lead to an increase in oxidative stress markers by variable degrees (Fig. 5). The phenolic derivative **3e** caused sharp elevation of malondialdehyde (MDA) to almost twice of its concentration in untreated cells, indicating large increase in the oxidative stress. In addition, **3e** caused extensive depression (about 10 fold) of the ROS scavengers catalase (CAT) and superoxide dismutase (SOD). The unsubstituted **3a** gave much weaker effects on all oxidative parameters. Furthermore, a test for superoxide anion radical ($O_2^{\cdot-}$) confirmed the above results of oxidative stress induction due to ROS accumulation. The amount of $O_2^{\cdot-}$ produced upon treatment of HCT116 cells with **3a** and **3e** was elevated (Fig. 6).

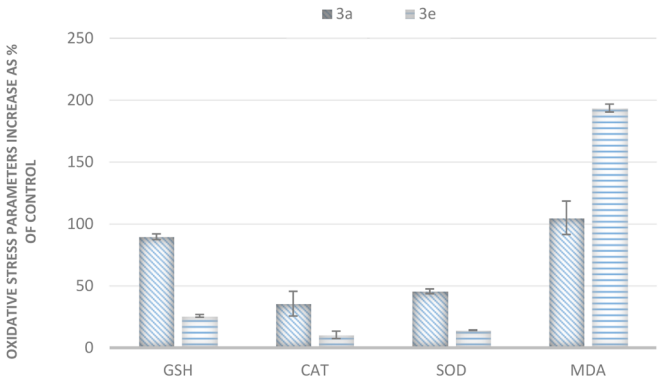

Fig. 5. Effect of Compounds **3a** and **3e** on Oxidative Stress Parameters (MDA, GSH, SOD, and CAT) in HCT116 Cells

The values are expressed as percentage of controls and calculated from the means of three independent experiments. (Color figure can be accessed in the online version.)

Immunofluorescence assays were performed to investigate the effect of **3a** and **3e** on the expression of cleaved-caspase 3. Treatment of HCT116 cancer cells with the IC_{50} of **3a** and **3e** significantly increased the expression and nuclear translocation of cleaved-caspase 3 (red) compared with non-treated cells (Fig. 7), indicating that our compounds halted the HCT116 growth and induced cellular apoptosis. These findings were further confirmed by the presence of typical morphological features of apoptotic nuclei including, 1-Chromatin

condensation (increase in cell membrane permeability and uptake of the fluorescent stain 4′,6′-diamidino-2-phenylindole (DAPI), leaving a stronger blue fluorescence), 2-Pyknosis, 3- The nuclear envelope becomes discontinuous and the DNA inside it is fragmented (karyorrhexis) which are the hallmark of apoptotic cells (Fig. 8).

Discussion

The results of both cytotoxicity and cell cycle analysis indicated that the 2-styryl-4-imidazolone scaffold (styryl group conjugated to an electron-withdrawing moiety) was a promising antiproliferative pharmacophore. In 39 cytotoxicity tests, 19 times the IC_{50} was at a low micromolar ($<5\,\mu M$) range. The advantage of the new compounds was highlighted by being safe on normal cells (compounds **3a** and **3e**) with IC_{50} values higher than $100\,\mu M$. It is worthy to mention that the 2-phenyl analogue of **3e** (5-benzylidene-3-(4-hydroxyphenyl)-2-phenyl-3,5-dihydro-4*H*-imidazol-4-one) was reported to be inactive against MCF7 cancer cell line[2] while our 2-styryl derivative **3e** exhibited good cytotoxicity ($IC_{50}=3.9\,\mu M$) against the same cell line. This underscores the importance of the 2-styryl group for the cytotoxic activities.

Even though some compounds (**3h**, **3l** and **3m**) showed proliferation inhibition activities (under $100\,\mu M$) against BHK and WI-38 cell lines, their selectivity index were still high against cancer cells over normal cells. This was interpreted based on selectivity that ranged from 8–25 times provided that IC_{50} values against cancer cell lines are $<10\,\mu M$. The structure–activity relationships (SAR) revealed that the antiproliferative potencies seemed less affected by the type of N3-substitution. The less clear SAR is usually complicated by pharmacokinetic factors in cell-based phenotypic screening.[26]

The cell cycle analysis of HCT116 cancer cells, but not MCF7, confirmed the similarity of cellular behavior of our compounds with that of BCA, a cinnamaldehyde analogue[23] (Fig. 1). BCA and our compounds **3a** and **3e** caused accumulation of cells in the pre-G phase. This cell cycle effect was confirmed by the presence of a pre-G peak in the cell cycle profile analysis and that may have resulted from degradation or fragmentation of genetic material, indicating a possible role for apoptosis in their cell growth inhibition activities. Moreover, compound **3a** induced a significant increase in the S-phase population with a concomitant decrease in the G0/G1 population, indicating S-phase arrest. Comparing the cell cycle effects of our compounds on HCT116 colon cancer cells and MCF7 breast cancer cells indicated that the mechanism of cytotoxic activities differ between the two cell lines. Therefore, we postulated that MCF7 cells might be killed by another mechanism other than ROS induction and could not pursue the investigation on ROS elevation markers on MCF7. We focused our subcellular studies on HCT116 cells and conducted several confirmatory tests to measure the pro-oxidant activities of our compounds on this type of cancer cells. In addition, the potent anticancer compounds **3h**, **3l** and **3m** that showed some cytotoxic activities against normal cell lines

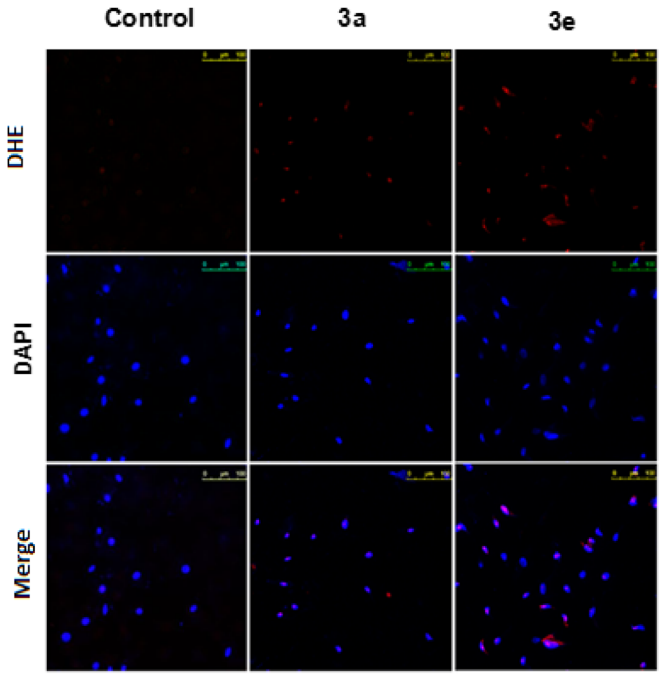

Fig. 6. Superoxide Free Radical Detection

Cells were grown on a cover slip in a 12 well plate for 24 h, then exposed to the IC_{50} of compounds **3a** and **3e** for 24 h. Cells then were incubated with $10\,\mu M$ dihydroethidium (DHE), at 37°C for 30 min and $1\,\mu M$ DAPI was used as counter stain. The cover slips were then mounted and visualized by Leica fluorescence microscope. Red fluorescence represents DHE staining in the top row and blue stain for DAPI in the middle row. (Color figure can be accessed in the online version.)

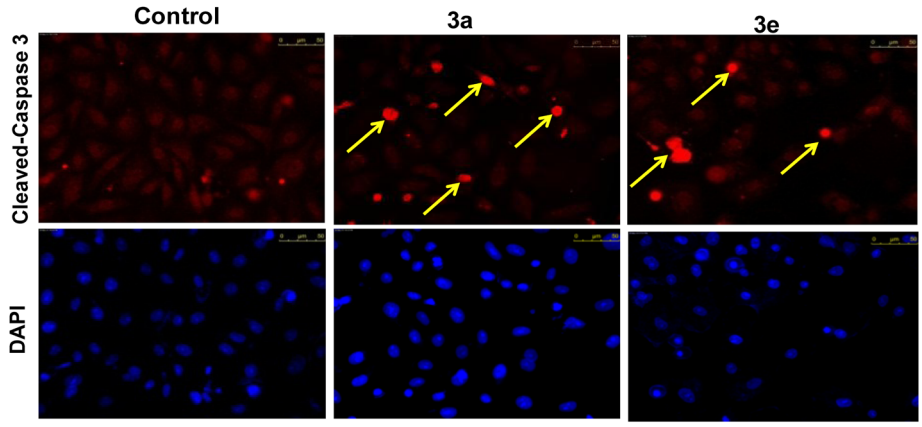

Fig. 7. Effects of **3a** and **3e** on the Cellular Expression and Nuclear Translocation of Cleaved-Caspase 3 in Human Colon Cancer Cells (HCT116)

Immunofluorescence staining of cleaved-caspase 3 expressions in human HCT116 cells treated for 24 h with **3a**, and **3e**. The cells were stained with DAPI to visualize nuclei (blue) and with Cy3-coupled secondary antibodies to visualize the distribution of caspase-3 (red). Scale bar, $50\,\mu m$. (Color figure can be accessed in the online version.)

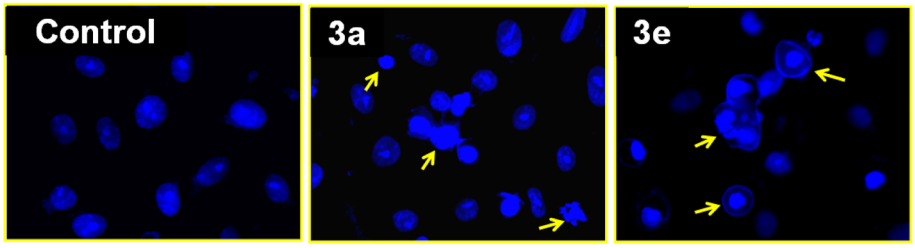

Fig. 8. Effects of **3a** and **3e** Treatment on the Nuclear Structures of HCT116 Cells

HCT116 cells were grown on cover slips and treated with **3a** or **3e**. Cells were incubated for 24 h and fixed in methanol/0.02% EDTA. The cells were stained with DAPI to visualize the nuclei. Treated cells show nuclear condensation and fragmentation along with the condensed blue fluorescence of DAPI. (Color figure can be accessed in the online version.)

(BHK and WI-38) were also excluded from mechanistic investigations.

In tracking the pro-oxidant effect of 2-styryl-4-imidazolone derivatives (**3a** and **3e**), we followed models from previous studies that focused on cellular markers of oxidative stress rather than isolated target screening as several pathways might be involved in producing higher oxidative stress inside the cancer cells.[27,28] Four cellular markers were selected here, the non-enzymatic glutathione (GSH, reduced marker) and malondialdehyde (MDA, oxidized marker) as well as redox enzymes catalase and SOD. The effect of the two potent compounds **3a** and **3e** on the ROS markers were significantly different. The *N*-(4-hydroxyphenyl) analogue **3e** consistently decreased the cellular activities associated with CAT and SOD. Moreover, it decreased the cellular level of GSH with concomitant increase in the lipid peroxidation product MDA. This indicates universal interruption in the cellular redox system, which is a hallmark of apoptosis.[29] The NH analogue **3a** induced only a slight increase in ROS parameters indicating a possible different cytotoxic mechanism than **3e**. Nonetheless, we found strong evidence for apoptotic cell death upon treatment of HCT116 cells by both compounds. Our observation of cleaved caspase 3 over expression and nuclear translocation after treatment by **3a** and **3e** within HCT116 cell offered another evidence of apoptosis induction *via* ROS generation. Cleaved caspase 3 induction of cell death is consistent with studies on tCA, BCA[21,23] (Fig. 1).

The morphological changes of HCT116 cell nuclei further confirmed the pro-apoptotic activity of compounds **3a** and **3e** (Fig. 7). The nuclear morphology shows chromatin condensation (evidenced by an increase in cell membrane permeability and uptake of DAPI), leaving a stronger blue fluorescence, pyknosis and karyorrhexis. All these features are considered as the hallmark of apoptotic cells.[30] All above mechanistic studies confirmed that the cytotoxic activities of **3a** and **3e** are similar but not identical between the two compounds. Compound **3e** clearly induces apoptotic changes *via* ROS induction. However, compound **3a** also induced cell apoptosis but it was not clear that ROS induction is the dominant factor in cell death.

Conclusion

In this work, we developed 4-imidazolone derivatives bearing 2-styryl group with fixed benzylidene sustituent on C-5 and variable substituents on N-3 as potent cytotoxic agents against colon, breast and hepatic cancer cell lines. Two compounds (**3a** and **3e**) could selectively inhibit cancer cell growth by the induction of oxidative stress similar to the styryl analogue BCA as revealed by several experiments on ROS markers, apoptotic markers and cell-cycle changes. This research is preceded by only few reports about the cancer cell inhibition profiles of 4-imidazolone derivatives especially in the area of ROS elevation. In the future, we are looking forward to further investigate the pharmacokinetics and establish a stronger pharmacological profile for the discussed compounds, including *in vivo* toxicity and efficacy studies. New variations could be introduced in the future to investigate the SAR of substitutions on the phenyl rings of the benzylidene and styryl moieties. Finally, the highly selective anticancer of potent compound with virtually no toxicity against normal cell lines is indeed encouraging to pursue these 4-imidazolone analogues for drug development.

Experimental

General All melting points were uncorrected and measured using the capillary melting point instrument BI 9100 (Barnstead Electrothermal, U.K.). Infrared spectra were recorded on a Thermo Scientific Nicolet iS10 Fourier transform (FT)-IR Spectrometer (King Fahd Center for Medical Research, King Abdulaziz University, Jeddah, Saudi Arabia). In this report, we only listed the important IR stretching bands, including NH, OH, CH, C=O, C=N and/or C=C. In FT-IR, all samples were measured neatly. ^{1}H-NMR spectra were determined on an AVANCE-III 600 MHz and AVANCE-III HD 850 MHz spectrometers (Bruker, Germany), and chemical shifts were expressed as ppm against TMS as an internal reference (King Fahd Center for Medical Research and Faculty of Science, King Abdulaziz University, Jeddah, Saudi Arabia). LC/MS analysis were performed on an Agilent 6320 Ion Trap HPLC-electrospray ionization (ESI)-MS/DAD (Santa Clara, CA, U.S.A.) with the following settings: The analytes were separated using an Macherey-Nagel Nucleodur-C18 column (150 mm length×4.6 mm i.d., 5 μm) (Macherey-Nagel GMBH & Co., KG, Duren, Germany). Mobile phase; isocratic elution using a mixture of isopropanol and 0.01 M ammonium acetate in water (65 : 35, v/v). The flow rate was 0.4 mL/min; total run time=20 min. Purities were reported according to percentage of Peak Areas at wavelength 280 nm. Microanalyses were operated using Vario, an Elmentar apparatus (Shimadzu, Japan), Organic Microanalysis Unit (Cairo University, Giza, Egypt) . Column chromatography was performed on a silica gel 60 (particle size 0.06–0.20 mm).

Chemical Synthesis The previously reported compounds cinnamoylglycine **1**,[31] azlactone **2**[32] and imidazolone derivatives **3a**,[33] **3b**,[34] and **3c**[32] were prepared according to procedures reported below, and their physical and spectral proper-

ties were confirmed. Purity of compounds were first assessed qualitatively using TLC, ^{1}H-NMR and quantitatively using LC/MS (UV detection at 254 nM). A compound was screened only if purity was confirmed to be above 95%.

(4*Z*)-Benzylidene-1-(4-fluorophenyl)-(2*E*)-styryl-5(4*H*)-imidazolone (**3d**)

A mixture of the oxazolone **2** (2 mmol, 0.554 g) and 4-fluoroaniline (2 mmol, 0.222 g) in acetic acid (10 mL) containing freshly fused sodium acetate (0.04 g, 0.5 mmol) was heated at 90°C with constant stirring for 6 h. Upon completion of the reaction, the excess acid was made alkaline with 10% $NHCO_3$ (30 mL) solution and extracted with EtOAc (2×25 mL). The combined organic extract was washed with water, then 1 M HCl (25 mL), followed by water and brine and then dried with Na_2SO_4. After solvent removal to dryness under reduced pressure, the residue was subjected to flash column chromatography (petroleum ether/DCM/MeOH. The product was isolated as an orange solid (0.622 g, 74%), mp 200°C. ^{1}H-NMR (600 MHz, $CDCl_3$) δ_H ppm 8.32 (2H, d, *J*=7.15 Hz), 8.09 (1H, d, *J*=15.81 Hz), 7.51–7.55 (3H, m), 7.50 (1H, s), 7.46 (1H, d, *J*=7.53 Hz), 7.38–7.43 (3H, m) 7.35 (2H, dd, *J*=9.03, 4.89 Hz), 7.25–7.30 (3H, m), 6.60 (1H, d, *J*=16.19 Hz); IR (FT-IR, cm^{-1}): 3065.7, 1708.7, 1622.6, 1508.4; LC-MS (ESI) retention time (RT)=11.5 min, *m/z* 369.3 $[M+H]^+$.

(4*Z*)-Benzylidene-1-(4-hydroxyphenyl)-(2*E*)-styryl-5(4*H*)-imidazolone (**3e**)

This compound was prepared according to the procedure described for the synthesis of **3d** starting from oxazolone **2** (2 mmol, 0.554 g) and 4-aminophenol (2 mmol, 0.218 g) as a greenish yellow solid (0.49 g, 65%), mp 286–289°C. ^{1}H-NMR (600 MHz, DMSO-d_6) δ_H ppm 8.38 (2H, d, *J*=7.5 Hz), 7.97 (1H, d, *J*=15.81 Hz), 7.64 (2H, m), 7.55–7.50 (2H, m), 7.48 (1H, m), 7.44–7.40 (3H, m), 7.21 (2H, m), 7.15 (1H, s), 6.94 (2H, m), 6.63 (1H, d, *J*=16.1 Hz); IR (FT-IR, cm^{-1}): 3322.3, 3027.7, 1691.3, 1617.6, 1506.19. LC-MS (ESI) RT=6.2 min, *m/z* 367.2 $[M+H]^+$. *Anal.* Calcd for ($C_{24}H_{18}N_2O_2$) C, 78.67; H, 4.95; N, 7.65; O, 8.73; found C, 78.98; H, 4.85; N, 7.48.

(4*Z*)-Benzylidene-1-(3-cyanophenyl)-(2*E*)-styryl-5(4*H*)-imidazolone (**3f**)

This compound was prepared according to the procedure described for the synthesis of **3d** starting from a mixture of the oxazolone **2** (2 mmol, 0.554 g) and the 3-aminobenzonitrile (2 mmol, 0.236 g) as a crystalline yellow solid (0.352 g, 47%), mp 227–228°C. ^{1}H-NMR (600 MHz, $CDCl_3$) δ_H ppm 8.32 (2H, d, *J*=7.5 Hz), 8.13 (1H, d, *J*=15.81 Hz), 7.81 (1H, dt, *J*=7.81 and 1.18 Hz), 7.73 (2H, m), 7.63 (1H, m), 7.57–7.51 (4H, m), 7.58 (1H, m), 7.44–7.41 (3H, m), 7.31 (1H, s), 6.57 (1H, d, *J*=15.8 Hz); IR (FT-IR, cm^{-1}): 3082.4, 2231.0, 1718.4, 1625.4, 1508.54. LC-MS (ESI) RT=9.0 min, *m/z* 376.3$[M+H]^+$.

(4*Z*)-Benzylidene-(2*E*)-styryl-1-(3-trifluoromethylphenyl)-5(4*H*)-imidazolone (**3g**)

This compound was prepared according to the procedure described for the synthesis of **3d**, starting from oxazolone **2** (2 mmol, 0.554 g) and 3-trifluoromethylaniline (2 mmol, 0.322 g). The product **3g** was isolated as a brownish red crystalline solid (0.622 g, 74%), mp 202–204°C. ^{1}H-NMR (600 MHz, $CDCl_3$) δ_H ppm 8.30 (2H, d, *J*=7.5 Hz), 8.12 (1H, d, *J*=15.81 Hz), 7.78 (1H, d, *J*=7.91 Hz), 7.73 (1H, t, *J*=7.72 Hz), 7.67 (1H, s), 7.58 (1H, d, *J*=7.53 Hz), 7.53 (4H, m), 7.47 (1H, m), 7.43–7.39 (3H, m), 7.31 (1H, s), 6.60 (1H, d, *J*=15.81 Hz); IR (FT-IR, cm^{-1}): 3060.4, 1710.3, 1625.4, 1510.1.

(4*Z*)-Benzylidene-1-(3-pyridyl)-(2*E*)-styryl-5(4*H*)-imidazolone (**3i**)

This compound was prepared according to the procedure described for the synthesis of **3d** starting from a mixture of the oxazolone **2** (2 mmol, 0.554 g) and the 3-aminopyridine (2 mmol, 0.188 g). The product **3i** was collected yellow solid (0.315, 44%), mp 222–223°C. The ^{1}H-NMR (600 MHz, $CDCl_3$) results were as follows: δ_H ppm 8.76 (1H, d, *J*=4.14 Hz), 8.67 (1H, s), 8.32 (2H, d, *J*=8.66 Hz), 8.14 (1H, d, *J*=15.81 Hz), 7.77 (1H, dd, *J*=10.54, 1.51 Hz), 7.57–7.51 (5H, m), 7.48 (1H, d, *J*=7.53 Hz), 7.41 (3H, d, *J*=4.14 Hz), 7.32 (1H, s), 6.61 (1H, d, *J*=15.81 Hz); IR (FT-IR, cm^{-1}) 3062.5, 1714.4, 1624.9, 1479.9; LC-MS (ESI), RT=6.5 min, *m/z* 352.3 $[M+H]^+$.

(4*Z*)-Benzylidene-1-(5-methylthiazol-2-yl)-(2*E*)-styryl-5(4*H*)-imidazolone (**3j**)

This compound was prepared according to the procedure described for the synthesis of **3d** starting from oxazolone **2** (2 mmol, 0.554 g) and 2-amino-5-methylthiazole (2 mmol, 0.228 g). The product **3j** was collected as a yellow crystalline solid (0.16 g, 21%), mp 144–145°C. ^{1}H-NMR (600 MHz, $CDCl_3$) δ_H ppm 8.32 (2H, d, *J*=7.15 Hz), 8.24–8.14 (2H, m), 7.71 (2H, d, *J*=6.78 Hz), 7.56–7.50 (2H, m), 7.50–7.41 (4H, m), 7.38 (1H, d, *J*=1.13 Hz), 7.32 (1H, s), 2.54 (3H, s); IR (FT-IR, cm^{-1}): 3052.8, 2977.7, 2919.1, 1713.5, 1636.0, 1513.64.

(4*Z*)-Benzylidene-(2*E*)-styryl-1-(1,3,4-thiadiazol-2-yl)-5(4*H*)-imidazolone (**5k**)

This compound was prepared according to the procedure described for the synthesis of **3d**, starting from oxazolone **2** (2 mmol, 0.554 g) and 3-trifluoromethylaniline (2 mmol, 0.202 g). The product was isolated as a yellow solid (0.197 g, 27%), mp 219–222°C. ^{1}H-NMR (600 MHz, $CDCl_3$) δ_H ppm 8.73 (1H, d, *J*=4.52 Hz), 8.65 (1H, d, *J*=1.88 Hz), 8.30 (2H, d, *J*=7.15 Hz), 8.12 (1H, d, *J*=15.81 Hz), 7.56–7.47 (4H, m), 7.45 (1H, d, *J*=7.15 Hz), 7.40–7.36 (2H, m), 7.31 (1H, s), 6.60 (1H, d, *J*=15.81 Hz).

(4*Z*)-Benzylidene-1-(furan-2-ylmethyl)-(2*E*)-styryl-5(4*H*)-imidazolone (**3l**)

This compound was prepared according to the procedure described for the synthesis of **3d**, starting from oxazolone **2** (2 mmol, 0.554 g) and furfurylamine (2 mmol, 0.177 mL). The product was isolated as a yellow solid (0.118 g, 16%), mp 145–147°C. ^{1}H-NMR (600 MHz, $CDCl_3$) δ_H ppm 8.29–8.23 (2H, m), 8.15 (1H, d, *J*=15.81 Hz), 7.66 (2H, dd, *J*=7.91, 1.13 Hz), 7.51–7.38 (7H, m), 7.22 (1H, s), 7.02 (1H, d, *J*=15.81 Hz), 6.39–6.34 (2H, m), 4.98 (2H, s); IR (FT-IR, cm^{-1}): 3065.2, 3030.4, 2955.9, 1705.5, 1625.7, 1508.2; LC-MS (ESI) RT=19.4 min, *m/z* 355.2 $[M+H]^+$.

(4*Z*)-Benzylidene-1-[2-(4-morpholinyl)ethyl]-(2*E*)-styryl-5(4*H*)-imidazolone (**3m**)

This compound was prepared according to the procedure described for the synthesis of **3d**, starting from oxazolone **2** (2 mmol, 0.554 g) and 2(4-morpholinyl)ethylamine (2 mmol, 0.262 mL). The product was isolated as a yellow solid (0.235 g, 30%), mp 186–187. ^{1}H-NMR (600 MHz, $CDCl_3$) δ_H ppm 8.27 (2H, d, *J*=7.53 Hz), 8.19 (1H, d, *J*=15.43 Hz), 7.74–7.66 (2H, m), 7.54–7.40 (6H, m), 7.19 (1H, m), 6.96 (1H, d, *J*=13.93 Hz), 3.96 (1H, br s), 3.72–3.69 (3H, m), 2.69–3.62 (4H, br m), 2.12 (4H, s); IR (FT-IR, cm^{-1}): 3032.1, 2926.17, 1689.3, 1626.0, 1512.8.

Biological Screening

Cell Culture

Human breast adenocarcinoma cell lines (MCF-7), human colon adenocarcinoma (HCT-116), human hepatocellular carcinoma (HepG-2), baby hamster kidney cells (BHK-21) and human lung tissue fibroblast (WI-38) were originally purchased from American type culture collection (ATCC, Wesel, Germany) and grown in the tissue culture lab of the Egyptian company for production of vaccines, sera and drugs (Vacsera, Giza, Egypt). The cells were transferred to our laboratory and maintained in Dulbecco Modified Eagle's medium (DMEM) or Roswell Park memorial Institute medium (RPMI1640) both are supplemented with 1% of 100 mg/mL of streptomycin, 100 units/mL of penicillin and 10% of heat-inactivated fetal bovine serum (Invitrogen, Carlsbad, CA, U.S.A.) in a humidified, 5% (v/v) CO_2 atmosphere at 37°C.

Cytotoxicity Assays

The SRB assays were performed according to Skehan *et al.*[18] Briefly, exponentially growing cells were trypsinized, counted and seeded at the appropriate densities (5000 cells/100 μL/ well) into 96-well microtiter plates. Cells were incubated in a humidified atmosphere at 37°C for 24 h. Then, the cells were exposed to different compounds at the desired concentrations, (0.01, 0.1, 1, 10, 100 and 1000 μM) or to 1% dimethyl sulfoxide (DMSO) for 72 h. At the end of the treatment period, the media were removed, and the cells were fixed with 10% trichloroacetic acid at 4°C for 1 h. The cells then were washed with tap water four times and incubated with SRB 0.4% for 30 min. Excess dye was removed by washing repeatedly with 1% (vol/vol) acetic acid. The protein-bound dye was dissolved in 10 mM Tris base solution for OD determination at 510 nm using a SpectraMax plus Microplate Reader (Molecular Devices, CA, U.S.A.). Cell viability was expressed relative to the untreated control cells and the IC_{50}s were calculated using Graph pad prism 5 software (GraphPad Software, Inc., CA, U.S.A.).

Cell Cycle Analysis

To analyze the DNA content by flow cytometry, different cell lines were seeded at a density of 2×10^6 cell/T75 flask for 24 h; then, the cells were exposed to different compounds at their IC_{50} concentration for 24 h. The cells were collected by trypsinization, washed with phosphate-buffered saline (PBS) and fixed in ice-cold absolute alcohol. Thereafter, cells were stained using Cycletest™ Plus DNA Reagent Kit (BD Biosciences, San Jose, CA, U.S.A.) according to the manufacturer's instructions. Cell cycle distribution was determined using a FACSCalibur flow cytometer (BD Biosciences, San Jose, CA, U.S.A.).

Effect on Redox Regulator Activities in HCT116 Cells

HCT116 cells were incubated with the IC_{50} of compounds **3a** and **3e** for 48 h. At the end of treatment period, cells were washed thrice with PBS, collected by trypsinization, total protein content were extracted by sonication in ice cold PBS in the dark, protein amounts were quantified using Bio-rad DC protein assay kit. Equal amount of protein lysate were used for determination of reduced GSH content,[35] the content of lipid peroxidation product, MDA,[36] enzymatic activities of CAT[37] and SOD.[38]

Effect on Superoxide Anion Radical Generation in HCT116 Cells

The superoxide anion ($O_2^{\cdot-}$) production was tested by dihydrethidium (DHE) staining within HCT116 cancer cells (Fig. 5). HCT116 cells were cultured on sterile cover slips (Harvard Apparatus, 22 mm^2) in a 6-well plate at a density of 2×10^5 cells/well. Cells were allowed to attach to the cover slips for 24 h in a humidified atmosphere at 37°C and 5% CO_2. The cells were then exposed to compounds **3a** and **3e** for 24 h. At the end of the exposure time, the growth medium was removed, followed by washing thrice with phosphate buffered saline (PBS). The cells were then incubated with the $O_2^{\cdot-}$ probe dihydroethidium (DHE), 10 μM, and the nuclear stain 4′,6-Diamidino-2-phenylindole, dihydrochloride (DAPI), 1 μM, for 30 min at 37°C. After incubation, cells were washed thrice with PBS, a drop of mounting medium was added to a slide, and the cover slips were inverted on the mounting medium and sealed. Different fields were captured at 20X magnification power using a fluorescent microscope (Leica DM 5500B).

Effect on Cleaved- Caspase 3 Protein Expression in HCT116 Cells

Cleaved caspase-3 rabbit monoclonal antibody (mAb) was purchased from Cell Signaling Technology (Cell Signaling Technology, MA, U.S.A.), A Cy3-conjugated goat anti-rabbit antibody was purchased from Jackson ImmunoResearch (West Grove, PA, U.S.A.). 4′,6′-Diamidino-2-phenylindole (DAPI) was purchased from Sigma-Aldrich (St. Louis, MO, U.S.A.).

HCT116 cells were cultured on 22-mm^2 sterile coverslips (Harvard Apparatus) in sterile six-well plates at a density of 2×10^5 cells/well. Cells were exposed to IC_{50} concentration of compounds **3a**, **3e** or 1% DMSO in fresh serum-free medium for 24 h. At the end of the exposure, cells attached to cover slips were washed with PBS and fixed with ice cold methanol/0.01% ethylenediaminetetraacetic acid (EDTA) for 20 min. After fixation, cells were blocked for 30 min at room temperature with 0.1% Triton X-100/PBS containing 5% bovine serum albumin (BSA), washed with PBS and incubated for 45 min with the primary antibody (diluted in 5% BSA/PBS/0.1% Triton X-100) as indicated. Following washing, the bound antibodies were detected by Alexa 488-conjugated goat anti-rabbit Cy3 secondary antibodies. To stain the nuclei, cells were incubated with DAPI, and the cells were mounted in Fluoromount G (Biozol) and analyzed with the Leica DM 5500 B fluorescence microscope (Leica, Buffalo Grove, IL, U.S.A.).

Acknowledgments This work was funded by the Deanship of Scientific Research (DSR), King Abdulaziz University (KAU), Jeddah, under grant No. (166-015-D1434). The authors, therefore, acknowledge with thanks DSR technical and financial support. We appreciate the efforts of Mr. Magdy Ghazy, Mr. Mohamed Elmehyawy (NMR Unit, King Fahd Center for Medical Research, KAU) and Mr. Ahmed Kammona (Faculty of Pharmacy, KAU) to perform NMR and LC-MS analyses of new compounds. We also appreciate the efforts of Mr. Amr El-Araby for reviewing and editing the manuscript.

Conflict of Interest The authors declare no conflict of interest.

References

1) Kumar D., Mariappan G., Husain A., Monga J., Kumar S., *Arabian Journal of Chemistry*, **10**, 344–350 (2017).
2) Bayoumi A. H., *Open J. Med. Chem*, **2**, 105–111 (2012).
3) El-Araby M. E., Omar A. M., Khayat M. T., Assiri H. A., Al-Abd

A. M., *PLOS ONE*, **12**, e0168938 (2017).
4) El-Araby M., Omar A., Hassanein H. H., El-Helby A. G., Abdel-Rahman A. A., *Molecules*, **17**, 12262–12275 (2012).
5) Kortiwala N., Patel J., Desai V. A., *Journal of Chemistry and Chemical Sciences*, **6**, 25–32 (2016).
6) Liao W., Hu G., Guo Z., Sun D., Zhang L., Bu Y., Li Y., Liu Y., Gong P., *Bioorg. Med. Chem*., **23**, 4410–4422 (2015).
7) Liu Y., Jiang C., Wu H., Wu P., Si M., Hu Y., Liu T., *Med. Chem.*, **9**, 938–946 (2013).
8) Okazaki T., Kikuchi K., Watanabe T., Suga A., Shibasaki M., Fujimori A., Inagaki O., Yanagisawa I., *Chem. Pharm. Bull.*, **46**, 777–781 (1998).
9) Sato H., Tsuda M., Watanabe K., Kobayashi J. i., Rhopaladins A., *Tetrahedron*, **54**, 8687–8690 (1998).
10) Baker D. D., Chu M., Oza U., Rajgarhia V., *Nat. Prod. Rep.*, **24**, 1225–1244 (2007).
11) Hong S. H., Ismail I. A., Kang S. M., Han D. C., Kwon B. M., *Phytother. Res.*, **30**, 754–767 (2016).
12) Ka H., Park H. J., Jung H. J., Choi J. W., Cho K. S., Ha J., Lee K. T., *Cancer Lett*., **196**, 143–152 (2003).
13) Wu S. J., Ng L. T., Lin C. C., *Clin. Exp. Pharmacol. Physiol.*, **31**, 770–776 (2004).
14) Chew E. H., Nagle A. A., Zhang Y., Scarmagnani S., Palaniappan P., Bradshaw T. D., Holmgren A., Westwell A. D., *Free Radic. Biol. Med.*, **48**, 98–111 (2010).
15) Wondrak G. T., *Antioxid. Redox Signal*., **11**, 3013–3069 (2009).
16) Richter C., Gogvadze V., Laffranchi R., Schlapbach R., Schweizer M., Suter M., Walter P., Yaffee M., *Molecular Basis of Disease*, **1271**, 67–74 (1995).
17) Wondrak G. T., Villeneuve N. F., Lamore S. D., Bause A. S., Jiang T., Zhang D. D., *Molecules*, **15**, 3338–3355 (2010).
18) Cabello C. M., Bair W. B. 3rd, Lamore S. D., Ley S., Bause A. S., Azimian S., Wondrak G. T., *Free Radic. Biol. Med.*, **46**, 220–231 (2009).
19) Wiseman R. W., Miller E. C., Miller J. A., Liem A., *Cancer Res.*, **47**, 2275–2283 (1987).
20) Muegge I., *Med. Res. Rev.*, **23**, 302–321 (2003).
21) Shin D. S., Kim J., Han D. C., Son K. H., Lee C. W., Kim H. M., Hong S. H., Kwon B. M., *Bioorg. Med. Chem. Lett.*, **17**, 5423–5427 (2007).
22) Mohamed M. S., Mahmoud R. K., Sayed A. I., El-Araby M. E., *Open Journal of Medicinal Chemistry*, **2**, 24–29 (2012).
23) Han D. C., Lee M. Y., Shin K. D., Jeon S. B., Kim J. M., Son K. H., Kim H. C., Kim H. M., Kwon B. M., *J. Biol. Chem*., **279**, 6911–6920 (2004).
24) Omar A. M., Mahran M. A., Ghatge M. S., Chowdhury N., Bamane F. H., El-Araby M. E., Abdulmalik O., Safo M. K., *Org. Biomol. Chem.*, **13**, 6353–6370 (2015).
25) Skehan P., Storeng R., Scudiero D., Monks A., McMahon J., Vistica D., Warren J. T., Bokesch H., Kenney S., Boyd M. R., *J. Natl. Cancer Inst.*, **82**, 1107–1112 (1990).
26) Wawer M. J., Li K., Gustafsdottir S. M., Ljosa V., Bodycombe N. E., Marton M. A., Sokolnicki K. L., Bray M.-A., Kemp M. M., Winchester E., Taylor B., Grant G. B., Hon C. S., Duvall J. R., Wilson J. A., Bittker J. A., Dančík V., Narayan R., Subramanian A., Winckler W., Golub T. R., Carpenter A. E., Shamji A. F., Schreiber S. L., Clemons P. A., *Proc. Natl. Acad. Sci. U.S.A.*, **111**, 10911–10916 (2014).
27) Raj L., Ide T., Gurkar A. U., Foley M., Schenone M., Li X., Tolliday N. J., Golub T. R., Carr S. A., Shamji A. F., Stern A. M., Mandinova A., Schreiber S. L., Lee S. W., *Nature* (London), **475**, 231–234 (2011).
28) Trachootham D., Alexandre J., Huang P., *Nat. Rev. Drug Discov.*, **8**, 579–591 (2009).
29) Simon H. U., Haj-Yehia A., Levi-Schaffer F., *Apoptosis*, **5**, 415–418 (2000).
30) Nagarsenkar A., Guntuku L., Guggilapu S. D., K. D. B., Gannoju S., Naidu V. G. M., Bathini N. B., *Eur. J. Med. Chem.*, **124**, 782–793 (2016).
31) Kiviranta P. H., Leppänen J., Rinne V. M., Suuronen T., Kyrylenko O., Kyrylenko S., Kuusisto E., Tervo A. J., Järvinen T., Salminen A., Poso A., Wallén E. A., *Bioorg. Med. Chem. Lett.*, **17**, 2448–2451 (2007).
32) Badr M. Z., El-Sherief H. A. H., Tadros M. E., *Bull. Chem. Soc. Jpn*., **55**, 2267–2270 (1982).
33) Mukerjee A., Joseph K., Homami S. S., Sanjayan G. *Indian Journal of Chemistry. Sect. B: Organic Chemistry, Including*, *Med. Chem.*, **32**, 973–974 (1993).
34) Pfleger R., Markert G., *Chem. Ber.*, **90**, 1494–1499 (1957).
35) Beutler E., Duron O., Kelly B. M., *J. Lab. Clin. Med.*, **61**, 882–888 (1963).
36) Satoh K., *Clin. Chim. Acta*, **90**, 37–43 (1978).
37) Claiborne A., "Catalase Activity, Handbook Methods for Oxygen Radical Research," ed. by R. Greenwald, CRC Press, Boca Raton, FL, 1985.
38) Nishikimi M., Appaji N., Yagi K., *Biochem. Biophys. Res. Commun*., **46**, 849–854 (1972).